ORIGINAL PAPER

Use of radiomics to differentiate left atrial appendage thrombi and mixing artifacts on single-phase CT angiography

Shadi Ebrahimian[1] · Subba R. Digumarthy[1] · Fatemeh Homayounieh[1] · Andrew Primak[2] · Felix Lades[3] · Sandeep Hedgire[1] · Mannudeep K. Kalra[1,4]

Abstract

To assess if radiomics can differentiate left atrial appendage (LAA) contrast-mixing artifacts and thrombi on early-phase CT angiography without the need for late-phase images. Our study included 111 patients who underwent early- and late-phase, contrast-enhanced cardiac CT. Of these, 79 patients had LAA filling defects from thrombus (n = 46, mean age: 72 ± 12 years, M:F 26:20) or contrast-mixing artifact (n = 33, mean age: 71 ± 13 years, M:F 21:12) on early-contrast-enhanced phase. The remaining 32 patients (mean age: 66 ± 10 years, M:F 19:13) had homogeneous LAA opacification without filling defects. The entire LAA volume on early-phase CT images was manually segmented to obtain radiomic features (Frontier, Siemens). A radiologist assessed for the presence of LAA filling defects and recorded the size and mean CT attenuation (HU) of filling defects and normal LAA. The data were analyzed using multiple logistic regression with receiver operating characteristics area under the curve (AUC) as an output. The radiologist correctly identified all 32 patients without LAA filling defects, 42/46 LAA with thrombi, and 23/33 contrast mixing artifacts. Although HU of LAA thrombi and contrast mixing artifacts was significantly different, with the lowest AUC (0.66), it was inferior to both radiologist assessment and radiomics (p = 0.05). Combination of radiologist assessment and radiomics (AUC 0.92) was superior to HU (0.66), radiomics (0.85), and radiologist (0.80) alone (p < 0.008). Radiomics can differentiate between LAA filling defects from thrombi and contrast mixing artifacts on early-phase contrast-enhanced CT images without the need for late-phase CT.

Keywords Radiomics · Left atrial appendage · CT · Thrombus · Mixing artifact

Abbreviations

IRB	Institutional review board
ECG	Electrocardiogram
CT	Computed tomography
LAA	Left atrial appendage
TEE	Trans esophageal echocardiography
HIPAA	Health Insurance Portability and Accountability Act
PACS	Picture archiving communication system
DICOM	Digital imaging and communications in medicine
GLCM	Gray level co-occurrence matrix
GLRLM	Gray level run length matrix

✉ Mannudeep K. Kalra
mkalra@mgh.harvard.edu

Shadi Ebrahimian
sebrahimian@mgh.harvard.edu

Subba R. Digumarthy
sdigumarthy@mgh.harvard.edu

Fatemeh Homayounieh
fhomayounieh@mgh.harvard.edu

Andrew Primak
andrew.primak@siemens-healthineers.com

Felix Lades
felix.lades.ext@siemens-healthineers.com

Sandeep Hedgire
hedgire.sandeep@mgh.harvard.edu

[1] Department of Radiology, Massachusetts General Hospital and Harvard Medical School, Boston, MA, USA

[2] Siemens Medical Solutions USA Inc., Malvern, PA 19355, USA

[3] Siemens Healthineers, Forchheim, Germany

[4] MGH Webster Center for Quality and Safety, Massachusetts General Hospital, Boston, MA, USA

GLSZM   Gray level size zone matrix
NGTDM   Neighboring gray tone difference matrix
GLDM   Gray level dependence matrix
ROC   Receiver operating characteristic
AUC   Area under the curve

Introduction

Atrial fibrillation (AF) is the most commonly diagnosed sustained cardiac arrhythmia in the United States and worldwide. Worldwide estimates suggest that about 33.5-million individuals suffered from AF in 2010 [1]. The United States' Centers for Disease Control and Prevention (CDC) estimated 2.7–6.1 million cases in 2010 with an expected burden of 12.1 million cases in 2020 [2]. In 2018, AF was stated on death certificates of 175,326 patients and described as the underlying cause of 25,845 deaths [1]. Thrombus formation in the left atrium is a major complication of AF associated with acute ischemic stroke or transient ischemic attacks with cardioembolic source [3]. Left atrial appendage (LAA) thrombus is also a contraindication for elective cardioversion of AF [4].

LAA is the most common location for thrombus formation in patients with AF. AF leads to loss of organized synchronous mechanical contractions of the LAA, and reduced LAA flow velocities, predisposing the thrombus formation [5]. Patients with multiple lobes and complex LAA morphology are more likely to develop LAA thrombus [6]. Unfortunately, slow blood flow that puts the patients with AF at risk of thrombus formation is also responsible for contrast mixing (pseudothrombus) artifacts on the early-phase, contrast-enhanced chest, and cardiac CT examinations. These artifacts can be challenging to differentiate from a true thrombus [7].

Most patients with suspected or known LAA thrombus undergo semi-invasive trans-esophageal echocardiography (TEE), a sensitive, specific, and ionizing radiation-free method of detecting thrombus. Prior studies report oropharyngeal, esophageal, gastric, and some miscellaneous complications following TEE [6]. In addition, due to the COVID-19 pandemic, the cardiac CT is the preferred method to TEE to reduce the rate of aerosolizing and disease transmission [8]. ECG-gated, non-invasive contrast-enhanced cardiac CT has a 96% sensitivity and 92% specificity for detecting LAA thrombus [9].

To differentiate LAA contrast mixing artifacts and thrombi, late phase CT images are acquired following initial early-phase contrast-enhanced CT images. If the filling defects resolve on the late-phase images, it is deemed as a contrast mixing artifact. Persistent filling defects are considered abnormal, with the most common cause being an LAA thrombus [9]. To ensure the acquisition of late-phase images in patients with filling defects on the early-phase images, imaging physicians and/or CT technologists need a quick assessment of the images to make a prompt decision for acquiring late-phase images, ideally within a minute. The need for prompt review and repeat acquisition can make it challenging to reduce radiation dose by limiting the scan range for late-phase to the region with filling defects. The LAA filling defect can change with a change in the timing of the delayed acquisition. In a study by Spagnolo et al., 15/63 patients (6%) had a persistent defect at 1 min, 12 patients (5%) at 3 min, and 10 (4%) at 6 min delay [10].

To avoid the need for the late-phase CT in these patients, we hypothesized that radiomics from early-phase, contrast-enhanced CT images could differentiate LAA mixing artifacts from thrombus. Radiomics obtains high-dimensional mathematical features from the digital medical images based on the intensity, shape, size, volume, and texture within a defined region of interest [11]. Previous studies have reported the successful characterization of lesions in different anatomic areas using radiomics [12, 13]. The purpose of our study was to assess if radiomics can differentiate between LAA contrast mixing artifact and thrombus on early-phase contrast-enhanced CT images without the need for late-phase.

Materials and methods

Need for informed consent for our retrospective institutional review board (IRB) approved and Health Insurance Portability and Accountability Act (HIPAA)-compliant study was waived. AP and FL are employees of Siemens Healthineers and did not take part in patient selection or data analyses. MKK has received research grants for unrelated projects from Siemens Healthineers and Riverain Tech. Other co-authors have no pertinent financial disclosure.

Patients

All 111 adult patients (mean age: 69 ± 12 years; 66 males, 45 females) underwent contrast-enhanced, ECG-gated coronary or pulmonary vein CT examinations. These patients were identified from a retrospective review of our Radiology Information System and picture archiving communication system (PACS; Agfa IMPAX-version 6.6.1.3004, Agfa-Gevaert Group). Based on the CT findings, patients were divided into those with LAA thrombus (n=46 patients; mean age: 72 ± 12 years, 26 males, 20 females), LAA contrast-mixing artifacts related to slow flow (n=33 patients; mean age: 71 ± 13 years, 21 males, 12 females), and those with homogenous contrast enhancement in LAA without thrombi or mixing artifacts (n=32 patients; mean age: 66 ± 10 years, 19 males, 13 females).

Patients with LAA filling defects, whether thrombi or mixing artifacts, and without late-phase CT acquisition through LAA were excluded. Patients with prior cardiac surgery and artifacts were excluded from the study (n = 43).

CT acquisition technique

All patients underwent contrast-enhanced CT examinations for clinically-indicated reasons such as pulmonary vein mapping, chest pain, equivocal stress test, and ascending thoracic aorta or dissection. All patients with LAA filling defects underwent electrocardiography (ECG)-gated cardiac CT on either a dual-source, second generation, 64-detector-row CT (n = 95 patients; Siemens Definition Flash, Siemens Healthineers, Forchheim, Germany) or single-source, 64-detector-row CT (n = 16 patients; GE Discovery 750 HD, GE Healthcare, Waukesha, Wis.) between July 2016 and March 2020. We selected consecutive patients without filling defects over the same time span. Patients received 60–80 mL of iodinated intravenous contrast (Iohexol 350, Omnipaque, GE Healthcare) at 4–6 mL/second via the antecubital vein. Scanning was triggered with bolus tracking technique with the region of interest in the proximal ascending thoracic aorta at the level of carina.

We used prospective ECG-triggered acquisition mode with automatic tube potential selection technique (Care KV, Siemens; KV Assist, GE) for imaging patients for pulmonary vein mapping CT and thoracic aorta CT angiography. Patients for coronary CT angiography were scanned with either prospective ECG-triggered or retrospective ECG-gated scan mode based on their heart rate and rhythm. We applied automatic tube potential selection mode and ECG-based tube current modulation with maximum tube current over the scanner-selected best systolic phase for scans performed with a retrospective ECG-gated acquisition. Images were reconstructed with a 0.625–0.75 mm section thickness and 0.5 mm section interval using a standard soft tissue reconstruction kernel and commercial iterative reconstruction techniques (ASIR, GE Healthcare for single-source CT; Safire, Siemens Healthineers for dual-source CT).

As per the standard of care in our hospital, early-phase contrast-enhanced images were reviewed on the scanner graphic user interface upon completing their reconstruction. In patients with filling defects in LAA, late-phase CT images were acquired through their hearts within one-minute of their early-phase CT images.

Both CT dose index volume – CTDIvol (32 cm phantom size) and dose length product – DLP were recorded separately for early-phase contrast-enhanced and late phases.

Subjective assessment

A cardiothoracic subspecialty radiologist reviewed the early-phase phase CT for the presence of LAA filling defects on the PACS workstation. When present, LAA filling defects were classified as thrombus or contrast mixing artifact on only early-phase contrast-enhanced images and then with late-phase images. The radiologist also measured CT attenuation values (Hounsfield Units, HU) and the size of LAA filling defects. In patients without LAA filling defect, CT attenuation values were measured in the contrast-opacified LAA on early-phase contrast-enhanced CT images.

Radiomic features

Deidentified thin-section CT image data were exported offline in digital imaging and communications in medicine (DICOM) format and processed with a standalone research radiomics prototype (FRONTIER, Siemens Healthineers) [14]. A post-doctoral research assistant (1-year experience) segmented the entire LAA in the early phase CT images with the manual segmentation tool. A free-hand ROI was drawn to segment the entire LAA volume. The prototype then calculated 1691 radiomic features from the segmented volume of interest (Fig. 1). Calculated radiomics comprised first-order, shape-based, and texture encoding features (n = 110), including the gray level co-occurrence matrix (GLCM), gray level run length matrix (GLRLM), gray level size zone matrix (GLSZM), neighboring gray-tone difference matrix (NGTDM), and gray level dependence matrix (GLDM). Besides these, the prototype calculated square, square root, logarithm, and exponential of the mentioned features (n = 372). To evaluate the spatial time–frequency of the two-dimensional images, 3-D wavelet transform parameters (n = 744) were used with the following subdivisions: HHH, HHL, HLL, HLH, LLH, LHL, LHH, LLL. Log with five (1.5 mm) sigma level (n = 465) of the radiomics classes was also retrieved. Further information on these radiomics is available on the following website (https://pyradiomics.readthedocs.io/en/latest/features.html accessed on October 28, 2020).

Statistical analysis

The extracted features were analyzed using built-in statistical tools in the same prototype. We used univariate statistics and multiple logistic regression tests with the area under the receiver operating characteristic (ROC) curve (AUC) as outputs. In order to determine the best model for multiple logistic regression analysis, the prototype first performs statistical significance using t-test/ANOVA for each feature. The p-values are corrected for
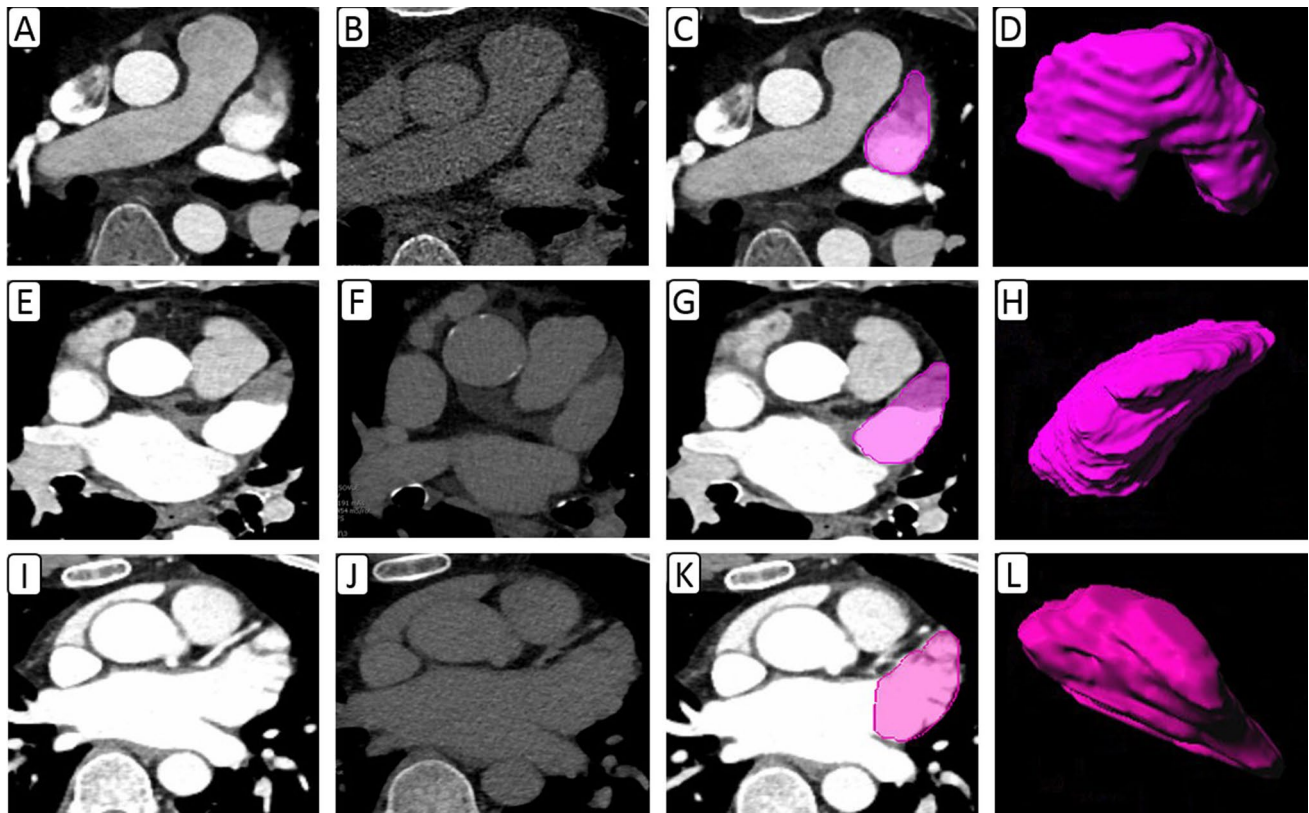
Fig. 1 Early-phase (**a**, **e**, **i**) and late-phase (**b**, **f**, **j**) transverse CT images of three patients including a 52-year-old male with LAA contrast mixing artifact (**a**, **b**), a 75-year-old male with a LAA thrombi (**e**, **f**), and a 63-year-old male with homogenous LAA opacification (**i**, **j**). Following manual segmentation of LAA (**c**, **g**, and **k**), the radiomics prototype created a three-dimensional volume of interest to estimate radiomics (**d**, **h**, and **l**)

multiple testing with Benjamini–Hochberg false discovery rate (FDR). Features with a corrected p-value of < 0.05 are considered statistically significant and selected for further analysis. For the remaining set of statistically significant features, a minimum redundancy maximum relevance (mRMR) feature selection is applied to eliminate irrelevant and redundant features. To keep the one-in-ten rule, we limited the mRMR feature selection to four features. With these resulting four features, a step-wise forward selection is applied. The best subset is selected using the Akaike information criterion (AIC). Separately, we assessed the performance of radiologist-measured HU and subjective classification of LAA filling defects (as thrombi or contrast mixing artifacts) on early-phase contrast-enhanced CT images with ROC analysis and compared them with radiomics using DeLong's test (IBM SPSS, version 26). One-way analysis of variance (ANOVA) was performed to compare age, gender, LAA volume, and size of filling defects in patients with and without LAA filling defects. A corrected p-value of 0.05 or less was considered as a statistically significant difference.

Results

There was no difference in age or gender distribution in patients belonging to the three subgroups (Table 1). The LAA volume in patients with contrast mixing artifacts was significantly higher than in patients with LAA thrombi or those without filling defects (Table 1) (p = 0.046). There was no significant difference in LAA volume in patients with thrombi and homogenous LAA opacification (p = 0.096). On early-phase, contrast-enhanced CT images, the radiologist correctly identified all 32 patients without filling defects in LAA, 42/46 LAA thrombi, and 23/33 patients with contrast mixing artifacts. Filling defects in 4/46 patients with LAA thrombi were labeled as contrast mixing artifacts, whereas 10/33 contrast mixing artifacts were deemed as thrombi on early-phase contrast-enhanced images.

The respective CTDIvol (mean ± standard deviation) for early and late phases were 14 ± 8 and 10 ± 6 mGy. Corresponding DLP for the two CT phases were 238 ± 162 and 166 ± 128 mGy.cm (p < 0.001).

LAA thrombi and contrast mixing artifacts

CT attenuation values, radiologist assessment, and radiomics enabled differentiation of LAA thrombi and contrast mixing artifacts with variable AUCs (Table 2). Although HU of LAA thrombi and contrast mixing artifacts were significantly different, with the lowest AUC (0.66), it was significantly inferior to both radiologist assessment and radiomics (p = 0.05). A combination of radiologist assessment and radiomics was superior to the AUCs of HU, radiomics, and radiologist alone (p < 0.008). A combination of radiomics including 3D wavelet-transform of size zone non-uniformity (GLSZM), log-sigma (1.5 mm) of small area emphasis (GLSZM), and a square of dependence variance (GLDM), had the highest AUC for differentiating mixing artifacts and thrombi (AUC: 0.85, p = 0.03) (Table 3). There was no change in the ability of radiomics (AUC 0.86, p = 0.004) for differentiating patients with LAA thrombi and contrast mixing artifacts when analyses was limited to exams performed on scanners one CT vendor (with exclusion of GE scanners, n = 16 patients).

Table 1 Distribution of patients in the three groups of patients included in the study

	Thrombus	Mixing artifact	Normal LAA	P-value
# Patients	46	33	32	–
Gender (M:F)	26:20	21:12	19:13	0.817
Age	72 ± 12 years	71 ± 13 years	66 ± 10 years	0.054
LAA volume	13.7 ± 6.9 mL	16.9 ± 9.1 mL	13.1 ± 6.9 mL	0.096
HU	66 ± 26	100 ± 51	405 ± 127	*
Size of filling defect	20 ± 7 mm	18 ± 5 mm	–	0.08
Radiologist assessment	Thrombus (42/46) Mixing artifact (4/46)	Mixing artifact (23/33) Thrombus (10/33)	32/0	*

M male, *F* female

*Variables assessed with ROC analysis

Table 2 Performance of HU, radiologist subjective assessment, and radiomics for differentiating LAA thrombi, contrast mixing artifacts and those without any thrombi (with normal LAA enhancement or mixing artifacts)

	Thrombus vs artifact		Thrombus vs no thrombus	
	AUC (95% CI)	P-value	AUC (95% CI)	P-value
HU	0.66 (0.54–0.79)	0.012	0.83 (0.75–0.91)	0.037
Radiologist assessment	0.80 (0.69–0.90)	< 0.001	0.89 (0.83–0.95)	0.031
Radiologist assessment + HU	0.79 (0.68–0.90)	< 0.001	0.89 (0.83–0.96)	0.032
Radiomics	0.85 (0.79–0.85)	0.03	0.87 (0.83–0.88)	0.02
Radiomics + Radiologist assessment	0.92 (0.86–0.98)	< 0.001	0.94 (0.90–0.98)	< 0.001

Combining radiologist assessment and radiomics yielded the best AUCs for both comparisons

Table 3 Best radiomic models for differentiating patients with LAA thrombi and contrast mixing artifacts as well as those with and without LAA thrombi

LAA thrombus vs contrast mixing artifact	AUC (95% CI)	P-value
Wavelet-size zone non uniformity (GLSZM) + Square-dependence variance (GLDM) + Log-sigma (1.5 mm)-small area emphasis (GLSZM)	0.85 (0.77–0.94)	0.03
Wavelet-size zone non uniformity (GLSZM) + Square-dependence variance (GLDM)	0.84 (0.75–0.93)	0.0001
Wavelet-size zone non uniformity (GLSZM)	0.79 (0.70–0.89)	< 0.0001
LAA with and without thrombus		
Wavelet-10th percentile (First order) + Log-sigma (4.5 mm)-Normalized size zone non uniformity (GLSZM) + Original-Imc1 (GLCM)	0.87 (0.80–0.93)	0.02
Wavelet-10th percentile (First order) + Log-Sigma (4.5 mm)-Normalized size zone uniformity (GLSZM)	0.86 (0.76–0.91)	0.01
Wavelet-10th percentile (First order)	0.83 (0.72–0.88)	< 0.0001

GLCM gray level co-occurrence matrix, *GLDM* gray level dependence matrix, *GLSZM* gray level size zone matrix

LAA with and without thrombi

A combination of radiologist assessment and radiomics had significantly higher AUC for differentiating patients with LAA thrombi from those with normal LAA opacification and mixing artifacts (p = 0.05). A combination of 3D wavelet-transform of first-order statistics, log-sigma (4.5 mm) of normalized size zone non-uniformity (GLSZM), and original of Imc1 (GLCM) had the highest AUC of 0.87 (p = 0.02) for differentiating LAA thrombi from LAA without a thrombus (Table 3) (Figs. 2 and 3). Performance of radiomics for

detecting LAA thrombi did not change (AUC 0.90, p = 0.03) when only one-vendor CT scanners were used (exclusion of GE scanners, n = 16 patients).

Discussion

Radiomics differentiates LAA thrombi from contrast mixing artifacts with respective AUCs of 0.85 and 0.92 without and with radiologist evaluation of filling defect. Our results compare favorably with a recent study from Chun et al.,

Fig. 2 Cluster map of radiomics for differentiating LAA thrombus from contrast mixing artifact (**a**) and for differentiating LAA thrombus from normal LAA (patients with either contrast mixing artifact or homogenous contrast enhancement) (**b**) with the list of top radiomics
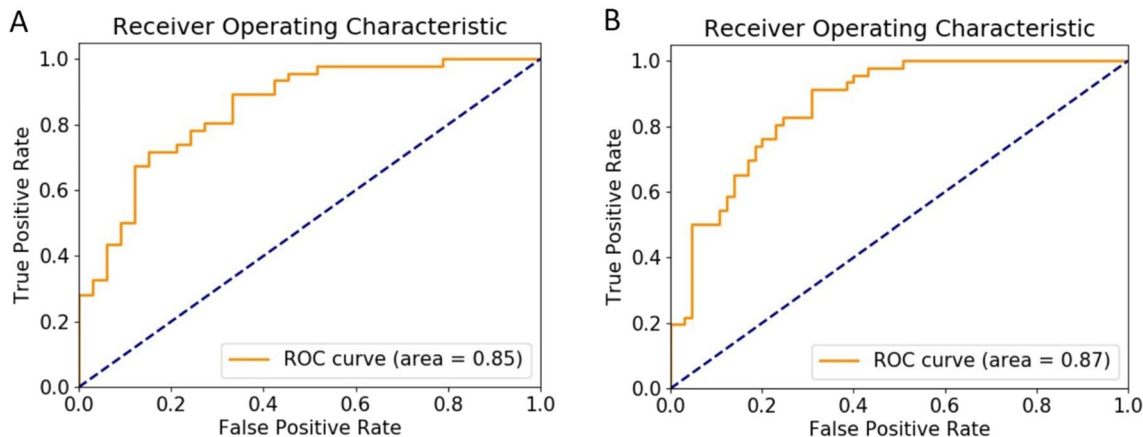

Fig. 3 Receiver operating characteristic curves for differentiating LAA thrombus from contrast mixing artifact (**a**) and for differentiating LAA thrombus from normal LAA (patients with either contrast

mixing artifact or homogenous contrast enhancement) (**b**) with the list of top radiomics

who reported an AUC of 0.78 for radiomics from the early contrast-enhanced phase [13]. Higher AUCs in our study was likely related to the use of a wider array of radiomics or segmentation over the whole LAA as opposed to segmentation and radiomics confined to the LAA filling defect in the prior study [13]. Another reason for the differential performance of radiomics between the two investigations might be difficulty in isolating small thrombi for radiomics in the prior study [13] compared to a larger volume of left atrial appendage that provides a larger volume of interest for radiomics in the current work.

Our study had a relatively symmetric distribution of LAA thrombi (n = 46 patients) and mixing artifacts (n = 33) as compared to the prior study with a skewed distribution of patients with artifacts (n = 70) than those with thrombi (n = 25) [13]. The combination of radiologist and radiomics had an AUC of 0.92 for differentiating LAA thrombi in our study, identical to 0.917 AUC in a recent study on a deep learning neural network trained with information on patients' gender and several other factors such as a history of myocardial infarction or heart failure, creatinine level, use of anticoagulants, LAA volume and linear dimensions related factors for predicting the probability of LAA thrombosis in patients with AF [15].

The mean HU of LAA had a low AUC (0.66) for differentiating LAA filling defects in our study instead of an AUC of 0.88 in a smaller study with 27 patients [16]. However, HU values in our study fared better than an AUC of 0.54 reported in a 95-patient study from Chun et al. [13]. These variations in AUCs can be related to heterogeneity in the patient population, contrast injection, scan, or reconstruction parameters for different CT examinations included in the three studies. However, such variations would also affect the performance of radiomics.

Our study's primary implication is that radiomics from the entire LAA with and without radiologist assessment can differentiate contrast mixing artifacts and thrombus. Such differentiation can help eliminate the need for late-phase images and reduce associated radiation dose. Mean CT attenuation values (HU) form the region of filling defect had much lower performance than radiomics. Although manual segmentation of LAA takes 1–2 min of processing time, in the future, machine learning algorithms can simplify and automate the segmentation of LAA from their current applications in the segmentation of multiple organs, including heart, lungs, and coronary arteries [17–20]. Radiation dose for late-phase CT can be reduced by limiting scan length to the LAA region, but this requires close monitoring of reconstructed images so that late phase acquisition is completed within 1 min of early-phase images. The radiation dose with the late-phase CT through LAA was 30% lower than the radiation dose for the entire cardiac CT (166 mGy.cm versus 238 mGy.cm) in our study.

There are limitations to our study. Our study was a retrospective analysis of single-center imaging data. Therefore, we could not include a larger sample size with equal distribution of patients in the three study groups. Our study is larger than a recent survey of radiomics in patients with and without LAA thrombus [13]. Another caveat pertains to the volume of interest over the entire LAA as opposed to a region of interest over the filling defect in prior studies [13]. We decided to use the entire LAA as a volume of interest since it was often challenging to segment an accurate region of interest to ill-defined filling defects in LAA, particularly with smaller thrombus and mixing artifacts. Our strategy might have resulted in better AUCs than reported in a prior study on radiomics confined to the region of interest with the filling defect [13]. We did not perform radiomics on CT images acquired in late-phase of contrast enhancement since we wanted to eliminate late-phase acquisition to reduce radiation dose and improve scanning efficiency. Finally, we used late-phase CT images as the standard of reference since several patients did not undergo transesophageal echocardiography or cardiac MRI. However, prior studies have reported the high accuracy of cardiac CT for detecting LAA thrombi [10, 21–23].

In conclusion, volumetric radiomics from the entire left atrial appendage can differentiate thrombi and contrast mixing artifacts from a single, early-phase contrast-enhanced cardiac CT without the need for late-phase images. Although our prototype automates the calculation and statistical analysis of radiomics, volumetric segmentation of the left atrial appendage requires additional effort and time. Future improvements in machine learning-based organ segmentation are needed to automate the process of LAA isolation fully.

Compliance with ethical standards

Consent to participate The need for the consent was waived due to the retrospective nature of the study.

References

1. National Center for Chronic Disease Prevention and Health Promotion, Division for Heart Disease and Stroke Prevention. https://www.cdc.gov/heartdisease/atrial_fibrillation.htm. Accessed 5 Dec 2020

2. Colilla S, Crow A, Petkun W, Singer DE, Simon T, Liu X (2013) Estimates of current and future incidence and prevalence of atrial fibrillation in the U.S. adult population. Am J Cardiol 112:1142–1147

3. Kamel H, Okin PM, Elkind MS, Iadecola C (2016) Atrial fibrillation and mechanisms of stroke: time for a new model. Stroke 47:895–900

4. https://www.ahajournals.org/doi/full/10.1161/circ.104.17.2118. Accessed 4 Nov 2020

5. Herring N, Page SP, Ahmed M et al (2013) The prevalence of low left atrial appendage emptying velocity and thrombus in patients undergoing catheter ablation for atrial fibrillation on uninterrupted peri-procedural warfarin therapy. J Atr Fibrillation 5(6):761. https://doi.org/10.4022/jafib.761

6. Hilberath JN, Oakes DA, Shernan SK, Bulwer BE, D'Ambra MN, Eltzschig HK (2010) Safety of transesophageal echocardiography. J Am Soc Echocardiogr 23:1115–1127

7. Saremi F, Channual S, Gurudevan SV, Narula J, Abolhoda A (2008) Prevalence of left atrial appendage pseudothrombus filling defects in patients with atrial fibrillation undergoing coronary computed tomography angiography. J Cardiovasc Comput Tomogr 2:164–171

8. Choi AD, Abbara S, Branch KR, Feuchtner GM, Ghoshhajra B, Nieman K, Pontone G, Villines TC, Williams MC, Blankstein R (2020) Society of cardiovascular computed tomography guidance for use of cardiac computed tomography amidst the COVID-19 pandemic endorsed by the American college of cardiology. J Cardiovasc Comput Tomogr 14(2):101–104

9. Romero J, Husain SA, Kelesidis I, Sanz J, Medina HM, Garcia MJ (2013) Detection of left atrial appendage thrombus by cardiac computed tomography in patients with atrial fibrillation: a meta-analysis. Circ Cardiovasc Imaging 6:185–194

10. Spagnolo P, Giglio M, Di Marco D, Cannaò PM, Agricola E, Della Bella PE, Monti CB, Sardanelli F (2020) Diagnosis of left atrial appendage thrombus in patients with atrial fibrillation: delayed contrast-enhanced cardiac CT. Eur Radiol. https://doi.org/10.1007/s00330-020-07172-2

11. Gillies RJ, Kinahan PE, Hricak H (2016) Radiomics: images are more than pictures, they are data. Radiology 278(2):563–577

12. Homayounieh F, Singh R, Nitiwarangkul C, Lades F, Schmidt B, Sedlmair M, Saini S, Kalra MK (2020) Semiautomatic segmentation and radiomics for dual-energy CT: a pilot study to differentiate benign and malignant hepatic lesions. AJR Am J Roentgenol 215:398–405

13. Chun SH, Suh YJ, Han K, Park SJ, Shim CY, Hong GR, Lee S, Lee SH, Kim YJ, Choi BW (2020) Differentiation of left atrial appendage thrombus from circulatory stasis using cardiac CT radiomics in patients with valvular heart disease. Eur Radiol. https://doi.org/10.1007/s00330-020-07173-1

14. Wels MG, Lades F, Muehlberg A, Suehling M (2019) General purpose radiomics for multi-modal clinical research. In: Medical imaging 2019: Computer-aided diagnosis, International Society for Optics and Photonics, p. 1095046

15. Suvorov A, Melik-Ogandzhanyan G, Dmitrieva E, Voskresenskaya N, Kruglov A (2020) Non-invasive risk assessment of the left atrial appendage thrombosis using deep learning methods. Eur Heart J Cardiovasc Imaging. https://doi.org/10.1093/ehjci/jez319.276

16. Hur J, Kim YJ, Lee HJ, Nam JE, Ha JW, Heo JH, Chang HJ, Kim HS, Hong YJ, Kim HY, Choe KO, Choi BW (2011) Dual-enhanced cardiac CT for detection of left atrial appendage thrombus in patients with stroke: a prospective comparison study with transesophageal echocardiography. Stroke 42:2471–2477

17. Homayounieh F, Pimgkun Y, Digumarthy S, Kruger U, Wang G, Kalra M 2020 Prediction of coronary calcification and stenosis: role of radiomics from Low-Dose CT. Academic Radiology

18. Jin C, Feng J, Wang L, Yu H, Liu J, Lu J, Zhou J (2018) Left atrial appendage segmentation using fully convolutional neural networks and modified three-dimensional conditional random fields. IEEE J Biomed Health Inform 22:1906–1916

19. Jin C, Feng J, Wang L, Yu H, Liu J, Lu J, Zhou J (2018) Left atrial appendage segmentation and quantitative assisted diagnosis of atrial fibrillation based on fusion of temporal-spatial information. Comput Biol Med 96:52–68

20. Leventić H, Babin D, Velicki L, Devos D, Galić I, Zlokolica V, Romić K, Pižurica A (2019) Left atrial appendage segmentation from 3D CCTA images for occluder placement procedure. Comput Biol Med 104:163–174

21. Kapa S, Martinez MW, Williamson EE, Ommen SR, Syed IS, Feng D, Packer DL, Brady PA (2010) ECG-gated dual-source CT for detection of left atrial appendage thrombus in patients undergoing catheter ablation for atrial fibrillation. J Interv Card Electrophysiol 29:75–81

22. Lazoura O, Ismail TF, Pavitt C, Lindsay A, Sriharan M, Rubens M, Padley S, Duncan A, Wong T, Nicol E (2016) A low-dose, dual-phase cardiovascular CT protocol to assess left atrial appendage anatomy and exclude thrombus prior to left atrial intervention. Int J Cardiovasc Imaging 32:347–354

23. Hur J, Kim YJ, Nam JE, Choe KO, Choi EY, Shim CY, Choi BW (2008) Thrombus in the left atrial appendage in stroke patients: detection with cardiac CT angiography–a preliminary report. Radiology 249:81–87